

The Thermal Investigation, Thermokinetic Analysis and Antimicrobial Activity of Two New Energetic Materials Obtained from Nucleophilic Substitution of Nitro Pyridine Ring

Emine Kübra İNAL¹, Nurcan ACAR², Şaziye Betül SOPACI³, Ceren YILDIZ⁴, Hasan NAZIR⁵, Orhan ATAKOL⁶, Sevi ÖZ^{7*}

^{1,2,4,5,6} Ankara University, Faculty of Science, Department of Chemistry, 06100, Ankara
^{3,7} Kırşehir Ahi Evran University, Faculty of Science and Arts, Department of Chemistry, 40100, Kırşehir

(Alınış / Received: 05.06.2018, Kabul / Accepted: 28.11.2018, Online Yayınlanma / Published Online: 25.12.2018)

Keywords

Energetic materials,
Thermal
decomposition,
Thermokinetic analysis,
Isoconventional-
nonisothermal
methods,
OFW,
KAS

Abstract: 2-Chloro-3 and 5-dinitropyridine were put into reaction with hydrazine and 3-aminopyrazole to obtain two new highly nitrogenous energetic substances. These energetic substances are; N(3,5-dinitropyridyn-2-yl) hydrazine (**I**), and N(3,5-dinitropyridyn-2-yl)3-aminopyrazole (**II**). These substances were characterized with element analysis, mass spectroscopy, IR spectroscopy, ¹HNMR and ¹³CNMR methods. Besides, the substances were analyzed with TG and thermal decomposition mechanisms were interpreted. Apart from these, isothermal and thermal kinetic analysis methods were used to reveal out the activation energies and Arrhenius pre-exponential factors. Thermodynamic parameters of decomposition reactions were measured by using these values. Nitrofuroxane ring was concluded to be the sub-product in thermal decomposition reactions. Gaussian 09 software algorithms were used to measure the standard formation enthalpy values of the two energetic substances. Using these values, the reaction enthalpy value of the thermal decomposition reaction according to Hess's law and the result obtained was compared with the value obtained from the differential scanning calorimetry method. Experimental and theoretical results were observed to be similar. In addition to these, antimicrobial effects of the highly nitrogenous energetic substances were measured for 5 different bacteria and their antifungal effects were measured for one type of fungus. As they were highly nitrogenous, the bacteria were found to be using the nitrogen in these substances for nutritional purpose.

Nitro Piridin Halkasının Nükleofilik Sübstitüsyonundan Elde Edilen İki Yeni Enerjik Malzemenin Termal İncelenmesi, Termokinetik Analizi ve Antimikrobiyal Aktivitesi

Anahtar Kelimeler

Enerjik malzeme,
Termal parçalanma,
Termokinetik analiz,
İzokonversiyonel-non
izotermal yöntemler,
OFW,
KAS

Özet: 2-Kloro-3,5-dinitropiridin, hidrazin ve 3-amimopirazol ile tepkimeye sokuldu ve iki yeni azotça zengin enerjik madde elde edildi, N(3,5-dinitropiridin-2-yl) hidrazin (I), ve N(3,5-dinitropiridin-2-yl)3-aminopirazol (II). Bu maddeler, element analizi, kütle spektroskopisi, IR spektroskopisi, ¹HNMR ve ¹³CNMR yöntemleri ile karakterize edildi. Bu maddeler TG ile incelendi ve termal parçalanma mekanizmaları yorumlandı. Bunun yanında izotermal ve nonizotermal kinetik analiz yöntemleriyle çalışıldı ve termal parçalanma tepkimelerinin aktivasyon enerjileri, Arrhenius pre-eksponansiyal faktörleri bulundu, bu değerler kullanılarak parçalanma tepkimelerinin termodinamik parametreleri hesaplandı. Termal parçalanma tepkimelerinde ara ürünün nitrofuroksan halkası olduğu sonucuna varıldı. Gaussian 09 yazılımı içindeki algoritmalar kullanılarak iki enerjik maddenin standart formasyon entalpisi değerleri hesaplandı. Bu değerler kullanılarak termal parçalanma tepkimesinin tepkime entalpisi değeri Hess yasası uyarınca hesaplandı ve bulunan sonuç Diferansiyel Taramalı Kalorimetre yönteminden elde edilen değer ile karşılaştırıldı, deneysel ve teorik sonuçların birbirinden uzak olmadığı görüldü. Bunlara ek olarak azotça zengin enerjik maddelerin antimikrobiyel etkileri 5 farklı bakteriye karşı, antifungal etkileri de bir mantar türüne karşı ölçüldü. Azotça zengin olduklarından bakterilerin bu maddelerdeki azotu besin olarak kullandığı belirlendi.

* Corresponding author: sevioz@hotmail.com

1. Introduction

As known, the nitro group is an electron attracting group. The nitro group is an electron attracting group with considerably high electronegativity value. [1]. For this reason, nucleophilic substitution takes place in the nitrated aromatic rings, not electrophilic substitution [2,3]. Picrylchloride is a pretty good example of this. Picrylchloride releases picrylamin with ammonia at room temperature as well as nucleophilic substitution reactions with picrylchloride; hydrazine, amino pyrazol, amino-1,2-4-triazol at hydrothermal conditions with the amino group [4-8]. In this study, 2-chloro-3,5-dinitropyridyne compound was put into reaction with two different nucleophiles and hydrazine and 3-aminopyrazole. Nucleophilic substitution was realized under hydrothermal conditions, scheme 1. As can be seen on Scheme 1, two new nitrogen-rich substances were produced. N (3,5-dinitropyridin-2-yl) hydrazine ($C_5H_5N_5O_4$, **I**) compound has about 3% and N (3,5-dinitropyridyne-2-yl) -3,5-dinitro-3-aminopyrazole ($C_8H_6N_6O_4$, **II**) compound has about 33.6% N in their structures. As we know, highly nitrogenous compounds are the primary substances involved in energetic substance researches. This is because the highly nitrogenous energetic substances are cleaner and more environmentally friendly energetic substances. These substances were characterized with element analysis, IR spectroscopy, mass spectroscopy, 1H NMR and ^{13}C NMR methods. Then the thermal decomposition reactions of all these compounds were analyzed through the thermogravimetric (TG) method.

It has long been known that poly nitro chloro benzenes easily undergo nucleophilic substitution reaction with amine groups [9-12]. In this way new energetic substances are produced. On the other hand, in the presence of ortho-substitute nitro groups, thermal decomposition of this energetic substance is through furoxane, scheme 2, [13-18].

The reaction given in Scheme 2 is the most prominent reaction to furoxane formation in the literature. If the amino group is attached instead of the azide group, the result is again the formation of the furoxane ring [4]. In this study, dinitro pyridine compound and heterocyclic compound were selected as the poly-nitro compound. Through TG, decomposition mechanisms of the compounds were studied and thermo-kinetic analysis measurements were made. Thermo-kinetic analysis measurements were used to measure the activation energies (E_a) of thermal decomposition reactions and the Arrhenius pre-exponential factor (A) values of these reactions. As we know, these thermo-kinetic values are a measure of the material's stability [19]. E_a and A values were used to measure the reaction enthalpy ($\Delta H_{\text{reaction}}$) values of thermal decomposition reactions, the entropy changes (ΔS) in these reactions and reaction

free energy ($\Delta G_{\text{reaction}}$) values. Theoretical standard formation enthalpy of the energetic molecules was measured using the programs in the Gaussian 09 package software. Standard formation enthalpies and theoretical standard formation enthalpies of possible decomposition reaction products were used to measure the reaction enthalpies of possible decomposition reactions according to Hess's Law. Reaction enthalpies of the experimental decomposition reactions of these substances were measured by the DSC device and the theoretical results were compared with the theoretical results.

Antimicrobial activity values of the two substances that were prepared with the intention to find out whether the tension of a molecule had biologic impacts or not, were experimentally defined for 5 bacteria and 1 fungus type and were interpreted.

2. Material and Method

The Thermal analysis studies, thermogravimetry (TG) and differential thermal analysis (DTA) were realized with Shimadzu DTG-60H apparatus. The all thermal analyses were measured in Pt pans at five different heating rates under nitrogen atmosphere. As is known, the TG method is not a suitable method for heat measurement. For this reason, the heats of thermal decomposition reaction of the energetic compounds were measured in DSC 50 differential scanning calorimetry device. The temperature and heat calibrations of both devices were made using In and Zn metals. The IR spectra of the energetic compounds were recorded at a resolution of 4 cm^{-1} by the use of Shimadzu Infinity model FTIR apparatus equipped with three reflection ATR unit. The element analysis of C, H and N were carried out by Eurovector 3018 CHNS model element analyzer device. For the NMR spectra of the energetic compounds were used Varian Brand Mercury model 400MHz NMR spectrophotometer. The 1H NMR and ^{13}C NMR spectra were taken in d_6 -DMSO. The molecular weights of the energetic materials were determined using Shimadzu 2010 Plus GCMS apparatus included Direct Inlet (DI) unit. The energetic substances were placed directly on the electron beam path with the aid of the DI unit and the mass spectra recorded.

Kinetic analysis studies were carried out using thermogravimetry at different heating rates for both compounds. For the N(3,5-dinitropyridyn-2-yl) hydrazine (compound I) was used 0.5, 0.8, 1.0 $^{\circ}C/min$. heating rate, while 2, 5, 10 $^{\circ}C.min^{-1}$ heating rate was used for the N(3,5-dinitropyridyn-2-yl)-3-aminopyrazol (compound 2).

The kinetic parameters of energetic compounds for the nonisothermal methods, KAS and OFW, were determined using the temperature at the 0.2- 0.4 - 0.5 - 0.6 and 0.8 $g(\alpha)$ values for all heating rates from the thermogravimetric curves. The activation energy and

pre-exponential factor values are calculated with the help of graphical methods using these determined temperature values according to the KAS and OFW methods. The results of Coats-Redfern method were obtained using the temperature values at each heating rate at the $g(\alpha) = 0.2, 0.4, 0.5, 0.6, 0.8$ values separately. For graphical calculations of KAS, OFW and CR methods were used the following formulas according to the literature. For KAS calculations equation 1 [20-29], for OFW equation 2 [22-32] and for CR equation 3 [31-34] were used respectively.

Equation 1.

$$\ln \frac{\beta}{T^2} = \ln \frac{A E a}{R g(\alpha)} - \frac{E a}{R T}$$

Equation 2.

$$\ln \beta = \ln \frac{0.0048 A E a}{R g(\alpha)} - 1.0516 \frac{E a}{R T}$$

Equation 3.

$$\ln \frac{g(\alpha)}{T^2} = \ln \left[\frac{A R}{\beta E a} \left(1 - \frac{2 R T}{E a} \right) \right] - \frac{E a}{R T}$$

But in most studies, because the term $1 - (2RT/Ea)$ in parenthesis is approximate ≤ 0.1 , the equation is used as below.

$$\ln \frac{g(\alpha)}{T^2} = \ln \frac{A R}{\beta E a} - \frac{E a}{R T}$$

In this equations β term shows heating rate as $^{\circ}\text{C} \cdot \text{min}^{-1}$, R term universal gas constant, Ea term activation energy of the thermal decomposition, A term Arrhenius pre-exponential factor of this thermal decomposition and T term the temperature as K . $g(\alpha)$ term determines fractional completed fraction of thermal decomposition reaction. These equations were written as accepting reaction order $n=1$ and considering realized as above mentioned. In three methods $\ln \beta$, $\ln[\beta/T^2]$ and $\ln[g(\alpha)/T^2]$ are plotted against $1/T$ values consequently Ea and A values were calculated using the above equations from slope and intercept values of the lines obtained.

Based on Ea and A values, some thermodynamic parameters in thermal reactions can be calculated easily. In most references, with the help of pre-exponential factor, the entropy change in thermal reaction can be calculated with

Equation 4.

$$\Delta S = 2.303 \left[\log \frac{A h}{k T} \right] R$$

equation as approximately. Beside this, as per the first rule of the thermodynamic, easily

Equation 5.

$$\Delta H = E a - R \Delta T$$

equation can be written and as per the Gibbs Free energy equation, from the equation 6, the Gibbs Free energy can be calculated, [19].

Equation 6.

$$\Delta G = \Delta H - T \Delta S$$

2.1. Theoretical calculation

The enthalpies (H) and free energies (G) were calculated using the CBS-4M method included in the Gaussian G09 W (revision D.01) software package [35-37]. The CBS-4M begins with a HF/3-21G(d) in order to structure optimization and zero-point energy calculations. It then uses a large basis set SCF and MP2/6-31+G calculations, as a base energy and to correct the energy through the second order respectively. A MP4(SDQ)/6-31+(d,p) calculation is used to approximate higher order contributions. [7, 38, 39].

Explosion products were estimated in accordance with literature data and using mass spectra. The formation enthalpies of these estimated products were determined from the literature or calculated using the same methods. Then, using these theoretical values according to the Hess law, the enthalpies of the 1st and 2nd thermal reactions were calculated.

$$\Delta H_{\text{Reaction}}^0 = \sum \Delta H_{\text{products}}^0 - \sum \Delta H_{\text{reactants}}^0 \quad (2)$$

Here, $\Delta H_{\text{Reaction}}^0$ is the theoretical reaction enthalpy, $\Delta H_{\text{products}}^0$ are the formation enthalpy of the products estimated or calculated, $\Delta H_{\text{reactants}}^0$ is the calculated formation enthalpy of energetic material.

2.2. Determination of biological activity

Besides the thermal investigations, the antibacterial effects of the prepared energetic substances were examined Three gram (-) (*Escherichia coli*, *Pseudomonas aeruginosa*, *Enterococcus faecalis* and two grams (+) (*Bacillus subtilis*, *Staphylococcus aureus*) bacterial strains were used for antibacterial assay, [36, 37]. In addition, we tested the energetic compounds against *C. albicans* as a pathogenic fungal strain. For bacterial strains Muller-Hinton agar (HMA) was used for bacterial growth and sabouraud dextrose agar (SDA) for *C. albicans*, [38]. Minimum inhibitory concentrations (MIC) for each microbial strain were calculated by agar dilution method. Fresh cultures prepared before 24 hours the test agar were used, which were also prepared with the chemical agent containing HMA to be tested. $10 \mu\text{L}$ bacterial suspension ($10^6 \text{ Cfu} \cdot \text{mL}^{-1}$ according to McFarland turbidity standard) of each strains were dropped on to the agar plates.

The MIC was determined with the fresh cultures after 24 h of incubation at 37°C and 24 h for *C. albicans*. The concentration range for chemicals was 512,0 – 8,0 mg.dm⁻³. Control antimicrobial tests of solutions were prepared in DMSO. Double serial dilutions were also prepared in the same solvent. The inoculated plates were incubated for 24 hours at 36°C for bacteria and for 48 hours at same temperature for the yeast. Positive controls (amoxicillin) were used to control the sensitivity of the tested bacteria, and amphotericin B were used as controls against the tested fungi.

2.3. Preparation of the energetic compounds

N(3,5-dinitropyridin-2-yl) hydrazine (**I**): 2.04 g (0.01 mole) 3,5-dinitro-2-chloropyridyne was dissolved in 50 mL MeOH by heating in a two necked flask. Then the solution was heated up to its boiling point under reflux. There was 0.60 g (0.012 mol) hydrazine hydrate added to it drop by drop. The mixture was heated under reflux for 4 hours and after this period was evaporated to the half volume. The dark brown product was filtered off and dried in air.

N(3,5-dinitropyridin-2-yl) hydrazine, C₅H₅N₅O₄, (**I**): Yield: %47-55.

Elemental Analysis: Expected %, C: 30.16; H:2.53; N:35,16

Found %, C: 29.81; H:2.27; N: 35,65

IR data (cm⁻¹): ν_{N-H} : 3348.42 – 3296.00 – 3271.27, $\nu_{C-H(Ar)}$: 3086.40, $\nu_{C=N}$: 1618.05, $\nu_{C=C(Ar)}$: 1581 – 1535.34, $\nu_{N=O}$:1319.31, $\delta_{C-H(Ar)}$:825.53 – 894.97.

m/z: 199 (molecular peak), 185 (base peak), 167, 155, 139, 137, 123.

¹H NMR data (δ ,ppm), in *d*₆-DMSO: 9.185 (H_{Ar}, pyridine ring), 8.884 (H_{Ar} pyrazole ring), 8.604 (-NH-), 7.21 (broad, NH₂)

¹³C NMR data (δ ,ppm), in *d*₆-DMSO: 151.34, 150.84, 148.97, 130.85, 129.75

N(3,5-dinitropyridin-2-yl)-3-aminopyrazole (**II**): 2.04 g (0.01 mole) 3,5-dinitro-2-chloropyridyne was dissolved in 50 mL MeOH by heating in a two necked flask. Then the solution was heated up to its boiling point under reflux. There was 0.83 g (0.01 mol) solution of 3-aminopyrazole in 20 mL hot MeOH added to it. It was heated under reflux for 4 hour evaporating up to two out of the three of its volume. The yellow product was filtered off and dried in air.

N(3,5-dinitropyridin-2-yl)-3-aminopyrazole,

C₈H₆N₆O₄, (**II**): Yield: % 60.

Elemental Analysis: Expected %, C: 38.41; H:2.41; N:33.58

Found %, C: 37.79; H:2.32; N: 32.46

IR data (cm⁻¹): ν_{N-H} : 3371.57 – 3307.92 – 3273.20, $\nu_{C-H(Ar)}$: 3143.83 – 3074.53

$\nu_{C=N}$: 1611.55, $\nu_{C=C(Ar)}$: 1593.20 – 1573.91, $\nu_{N=O}$:1321.24, $\delta_{C-H(Ar)}$:786.90 – 748.45.

m/z: 250 (molecular peak, (base peak), 204, 158, 131, 104, 94, 71, 57, 43.

¹H NMR data (δ ,ppm), in *d*₆-DMSO: 12.76 (-NH-), 10.60 (NH, pyrazole ring), 9.295 – 9.018 (H_{Ar} pyridine ring), 7.747 – 6.734 (H_{Ar} pyrazole ring).

¹³C NMR data (δ ,ppm), in *d*₆-DMSO: 150.47, 149.93, 145.40, 134.79, 130.87, 129.54, 126.98, 98.31

3. Results

No-I and **No-II** energetic substances' TG-DTA curves recorded at 10 and 25 °C.min⁻¹ heating rate are given in Figure 1a-f. Figures 1a, 1b, 1c and 1d show that energetic substance No-I is decomposed at single step with an exothermic reaction at around 175-200°C. As temperature increases, the energetic substance is observed to act like an explosive substance. Figures 1a and 1b show temperature-related DTA change and loss of mass heat whereas Figures 1c and 1d show time-related DTA change and loss of mass. Note that in Figures 1a and 1b, there is a sudden increase and decrease in temperature due to exothermic reaction, which can lead to a negative sloping in TG curves and irregular hysteresis in DTA curves. The reason for this is that, the rate of reaction is too high. Gas products that are produced at high rate absorb the reaction temperature and quickly leave the environment. Thus, rapidly formed gas products rapidly move away from the pan and in this short time the gas products removed the absorbed reaction enthalpy and consequently cool down around the pan for a short time. Therefore, the negative expected slope is positive in this part of the TG curve and DTA curves become abnormal, rather than Gaussian type curves. In this case, it is not possible to working with Ozawa and related OFW thermokinetic methods (Equation 2). This anomaly cannot be seen on the curves at the time scale. For this reason, TG-DTA curves of energetic substances No I is given using two different scales, Figures 1a-d. In energetic substance No II, the reaction is not so fast but slower and we can see from the curves on the temperature scale that the decomposition reaction is of two steps.

It can be seen on Figure 1 that, at 10 and 25°C. min⁻¹ heating rates, the energetic substance No. I is decomposed with a single step reaction whereas the energetic substance No. II is decomposed with a two-step reaction. As given in Scheme 2, aromatic amines or azides carrying nitro group at ortho position can be easily decomposed to furoxane ring. This is observed with numerous studies in the literature [13 – 17]. Furthermore, it is reported that, if a substituent is attached, via amino bridge, to the aromatic rings involving nitro group at ortho position, decomposition reaction again resembles the furoxane mechanism [4, 43, 44]. In the same studies, N (2,4,6-trinitrophenyl) hydrazine is reported to be similarly decomposed at around 190°C. 10 and 25°C. min⁻¹ heating rates can be high heating rates for explaining the decomposition mechanism of the energetic substance No I. The energetic substance No I is found to have two-step reaction at 10 °C.min⁻¹ heating rate, when measured with DCS, Figure 2.

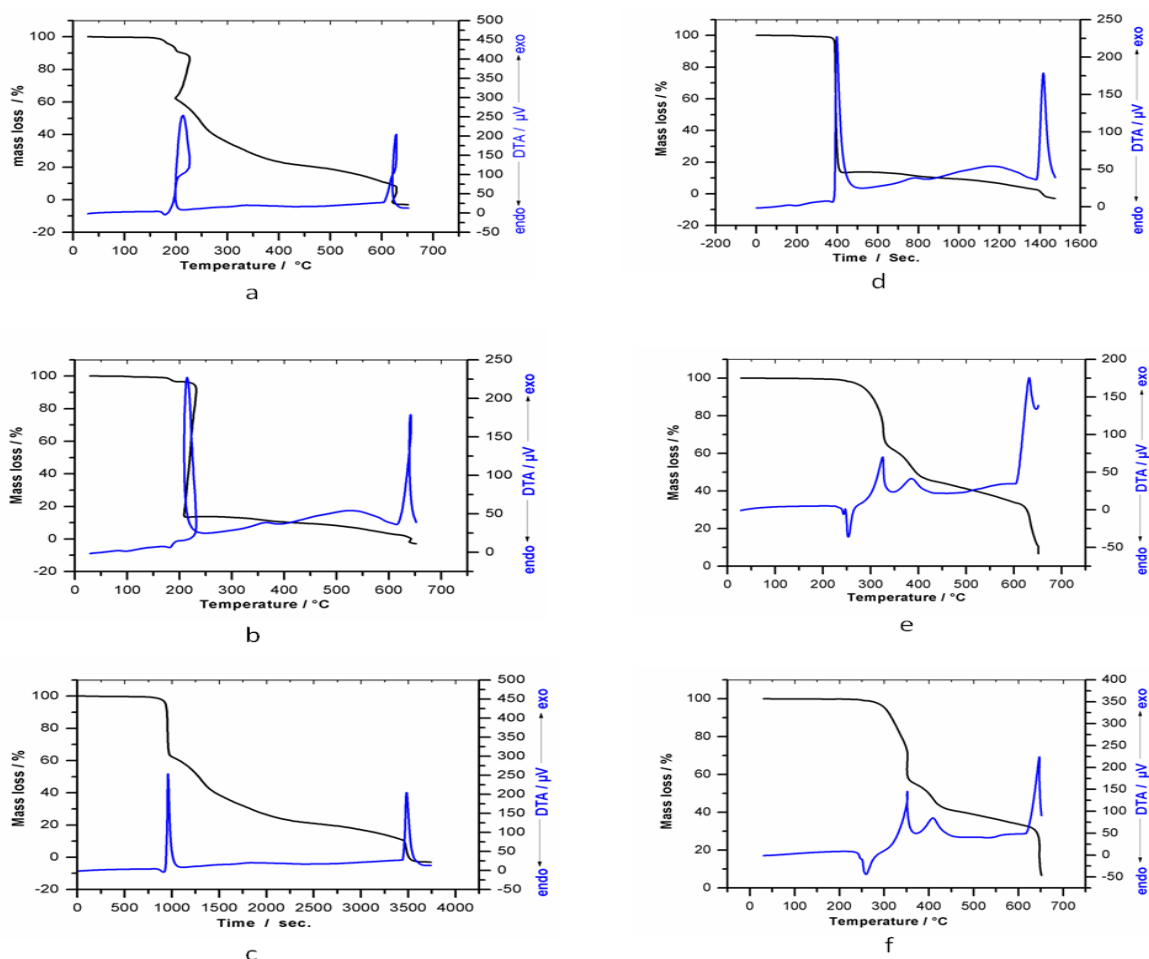


Figure 1. TG-DTA curves of **I** and **II** **a:** Temperature-TG-DTA curve of **I**, $10^{\circ}\text{C. min}^{-1}$ heating rates **b:** Temperature-TG-DTA curve of **I**, $25^{\circ}\text{C. min}^{-1}$ heating rates **c:** Time-TG-DTA curve of **I**, $10^{\circ}\text{C. min}^{-1}$ heating rates **d:** Time-TG-DTA curve of **I**, $25^{\circ}\text{C. min}^{-1}$ heating rates **e:** Temperature-TG-DTA curve of **II**, $10^{\circ}\text{C. min}^{-1}$ heating rates **f:** Temperature-TG-DTA curve of **II**, $25^{\circ}\text{C. min}^{-1}$ heating rates

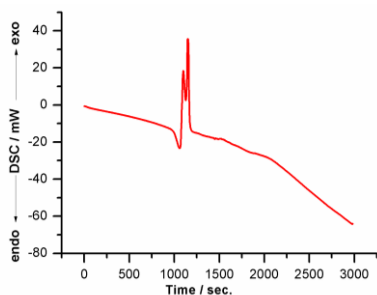


Figure 2. DSC curve of the energetic material **I** at $10^{\circ}\text{C. min}^{-1}$ heating rate

Thus, lower heating rates were used for the energetic substance No I and two-step reaction was obtained for TG curves. Figure 3a shows the DTA curve of the energetic substance No I at $0.8^{\circ}\text{C. min}^{-1}$ heating rate and Figure 3b shows the TG curve of the same substance. Figure 4 shows 3D drawing of DTA curves recorded at 0.5, 0.8, 10.0, 15.0, 20.0, and $25.0^{\circ}\text{C. min}^{-1}$ heating rates. Figures 1-4 show that both substances are decomposed with two-step sequential reactions similarly. Only the energetic substance No I appears to be single step at high heating rates, as it has a faster thermal decomposition reaction. In this case, a furoxane-like ring formation can be offered in parallel with the literature, Scheme 3.

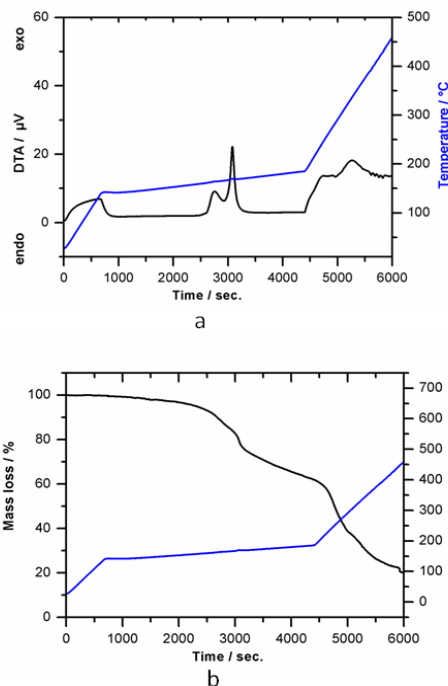


Figure 3. **a:** DTA curve of energetic material **I** at $0.8^{\circ}\text{C. min}^{-1}$ heating rate, **b:** TG curve of energetic material **I** at $0.8^{\circ}\text{C. min}^{-1}$ heating rate. Between 140-190 $^{\circ}\text{C}$ were recorded at $0.8^{\circ}\text{C. min}^{-1}$ heating rate on both curves.

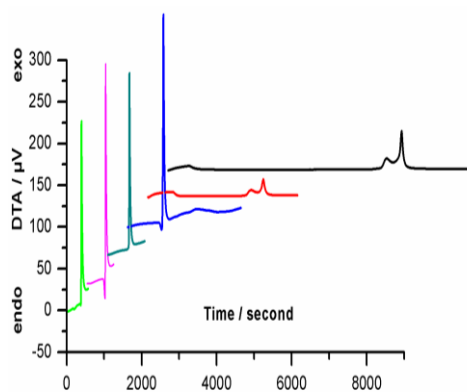
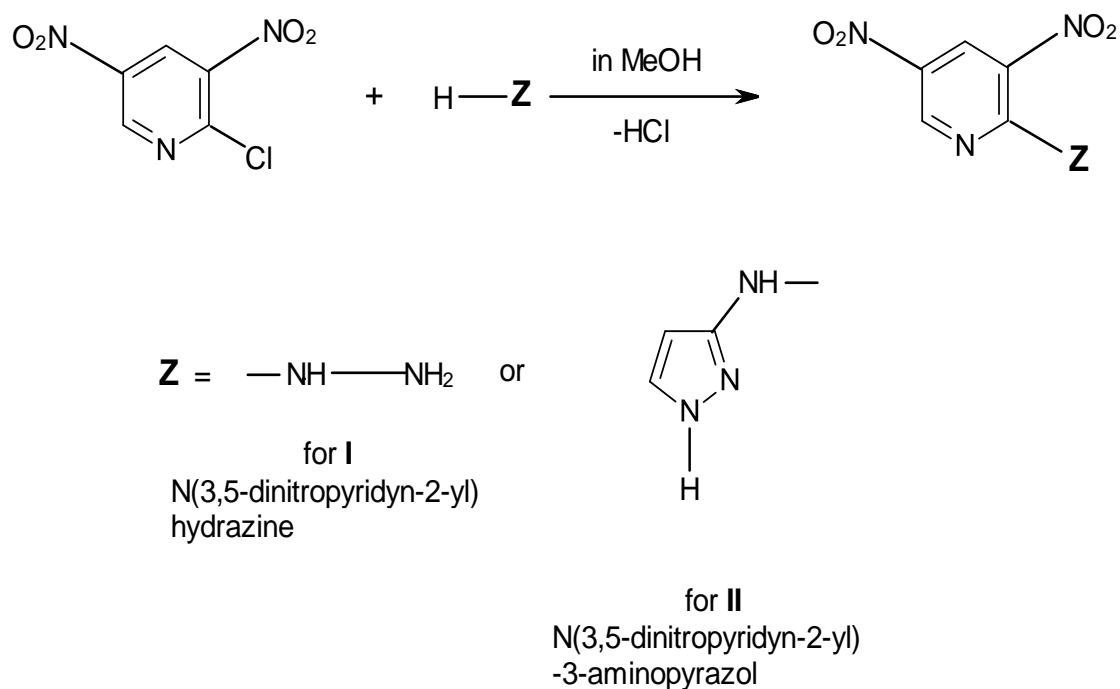
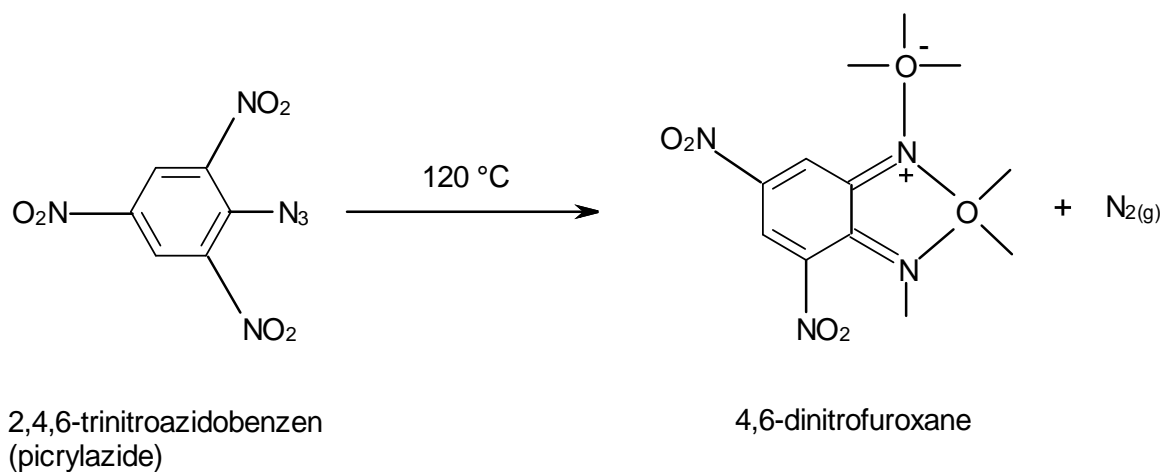


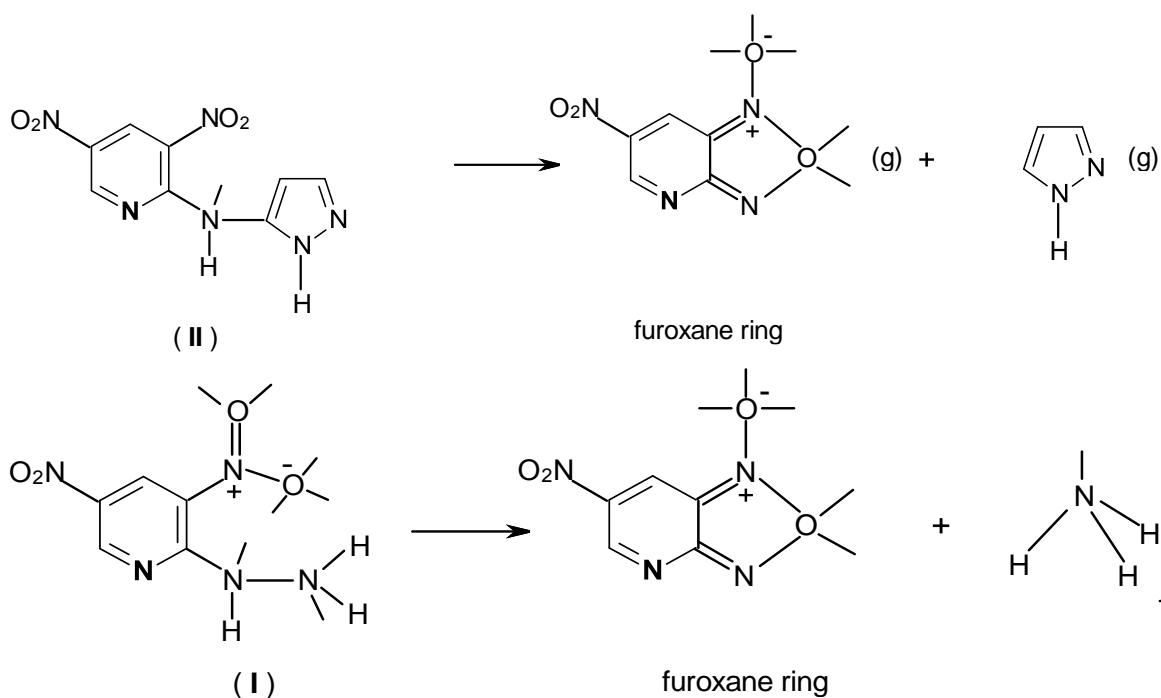
Figure 4. 3D plotting of DTA curves of energetic material I at the heating rate between 0.5 – 25.0 °C.min⁻¹



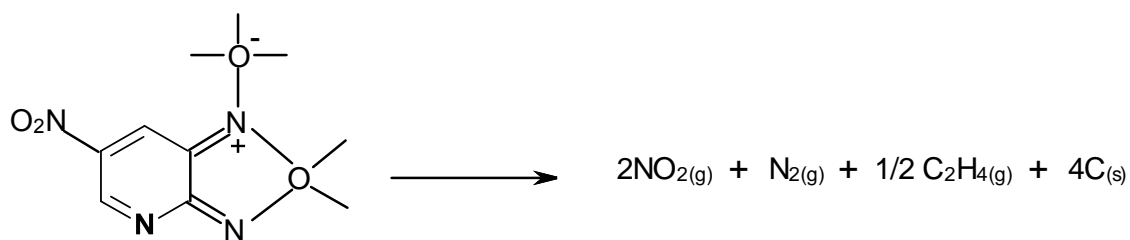
Scheme 1. The nucleophilic substitution reaction used of the preparation of the energetic materials



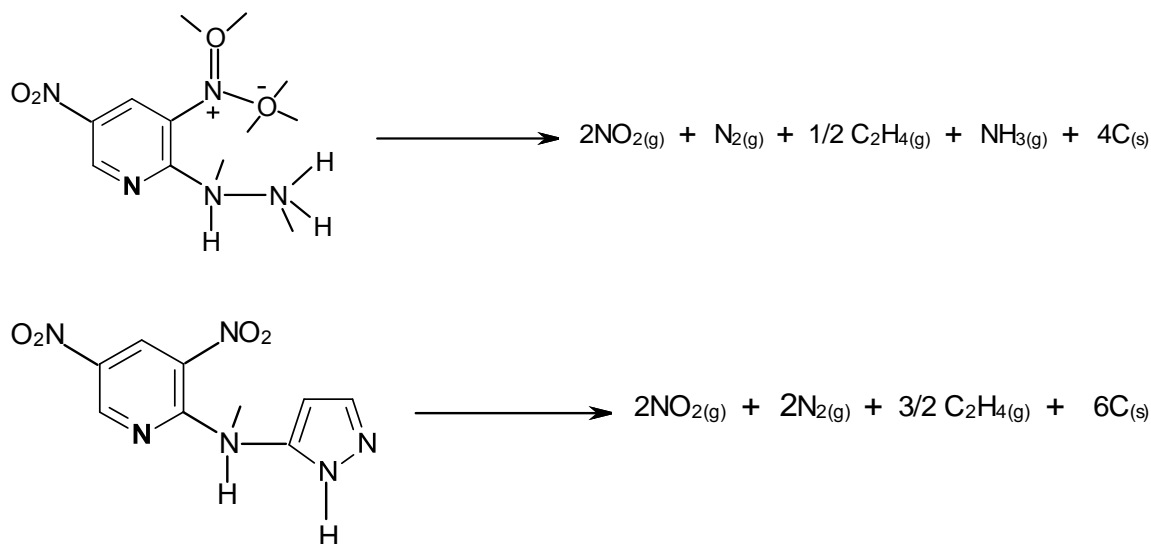
Scheme 2. First thermal decomposition reaction of picrylazide



Scheme 3. First step the suggested thermal decomposition of both energetic materials



Scheme 4. The thermal decomposition of the intermediate product furoxane similar product, second step.



Scheme 5. Total thermal decomposition reactions of both energetic materials

The furoxane compound then continues to decompose thermally. The reaction we could offer about the thermal decomposition of this substance at the end of DSC studies are given in Scheme 4. In this case, the most probable thermal decomposition reactions must be as given in Scheme 5 according to the results of DSC.

Theoretical and experimental reaction heat values found according to Hess's Law based on the thermo-analytical data and the measured formation enthalpy values of the two energetic substances are shown in Tables 1 and 2.

Table 1. The thermoanalytical data of the energetic materials prepared

Energetic Material	1. thermal reaction (first step)			2. thermal reaction		
	Temperature Range / °C	Mass loss %		Temperature Range / °C	Mass loss %	
		Calculated	found		calculated	found
C ₅ H ₅ N ₅ O ₄ , N(3,5-dinitro-2-pyridyl)hydrazine (I)	149.75 - 169.14	8.54	8.43±0.57	169.14 - 207.06		34.08±3.82
C ₈ H ₆ N ₆ O ₄ , 2-N(pyrazol-3-yl)amino-3,5-dinitropyridyne(II)	251.12 - 324.29	27.18	32.07±0.42	324.29 - 432.27		20.05±0.34

Table 2. The formation enthalpy values and calculated reaction enthalpies values and experimental measured reaction heat using DSC device

Energetic Material	The Theoretical Calculated Formation enthalpy value using Gaussian 09 / kJ/mol	The Estimated reaction products as written in scheme 5 or 6.	The Calculated theoretical reaction enthalpy values/ kJ/mol	The Measured reaction heat using DSC (Corrected value by adding Work against outer pressure. kJ/mol)
C ₅ H ₅ N ₅ O ₄ , N(3,5-dinitro-2-pyridyl)hydrazine (I)	207.92	NO _{2(g)} , C ₂ H _{4(g)} , N _{2(g)} , C _(s)	-161.42	-134.88
C ₈ H ₆ N ₆ O ₄ , 2-N(pyrazol-3-yl)amino-3,5-dinitropyridyne (II)	264.34	NO _{2(g)} , C ₂ H _{4(g)} , N _{2(g)} , C _(s)	-119.56	-108.81

Reaction values that are measured and experimentally found are not too close to each other but are at comparable size. The oxygen balance (Ω) rule generally applies to the decomposition of energetic substances. Measurements are done according to this rule [45, 46]. But this rule doesn't always apply. There are contrary examples, as well. The structure of the molecule and the interaction among the particles play a role in explosion reaction products [16, 44]. As the results are comparable, it must be noted that the theoretical program was successful.

Both energetic substances are decomposed in two steps as can be seen in Figures 1-4, but their rates are different. Particularly the energetic substance No I decomposes quite fast. For this reason, kinetic analysis was also performed in this study. As stated above, kinetic analysis was performed with isothermal (Coats-Redfern method, CR) two non-

isothermal (Kissinger-Akahira-Sunose method, KAS and Ozawa-Flyn-Wall method, OFW) methods. On the other hand, as can be seen on Figure 1a and Figure 1b, the energetic substance No. I gives explosion reaction at 10 or 25°C.min⁻¹ heating rates and when mass loss is shown in graphics against temperature, DTA curve and TG curve show anomaly. The slope is positive on TG curve, which makes calculation impossible. Thus, kinetic study for the substance No I was performed at 0.5, 0.8 and 1.0 °C.min⁻¹ heating rates only and numerical value could only be obtained for the 1st step of thermal decomposition. The first step of the energetic substance No I. could be measured with CR and KAS methods only. This is because when log β value is lower than 1.0°C.min⁻¹ value in OFW equation, the result obtained is negative, which makes measuring impossible, Figure 5a. The graphics obtained for the two energetic substances with OFW, KAS and CR methods are given in Figures 5 and 6.

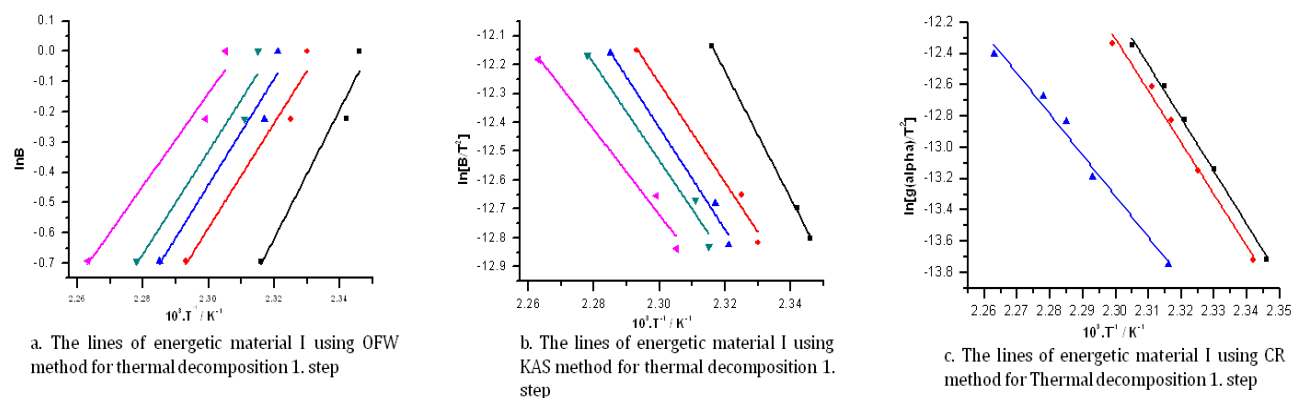


Figure 5. The lines obtained from the data of energetic material I for 1. thermal decomposition step using OFW, KAS and CR methods. In the drawing a and b, black: $g(\alpha)=0.2$, red: $g(\alpha)=0.4$, blue: $g(\alpha)=0.5$, green: $g(\alpha)=0.6$, pink: $g(\alpha)=0.8$, in figure c black: heating rate: 0.5 °C.min⁻¹, red: heating rate: 0.8 °C.min⁻¹, blue: heating rate: 1.0°C.min⁻¹

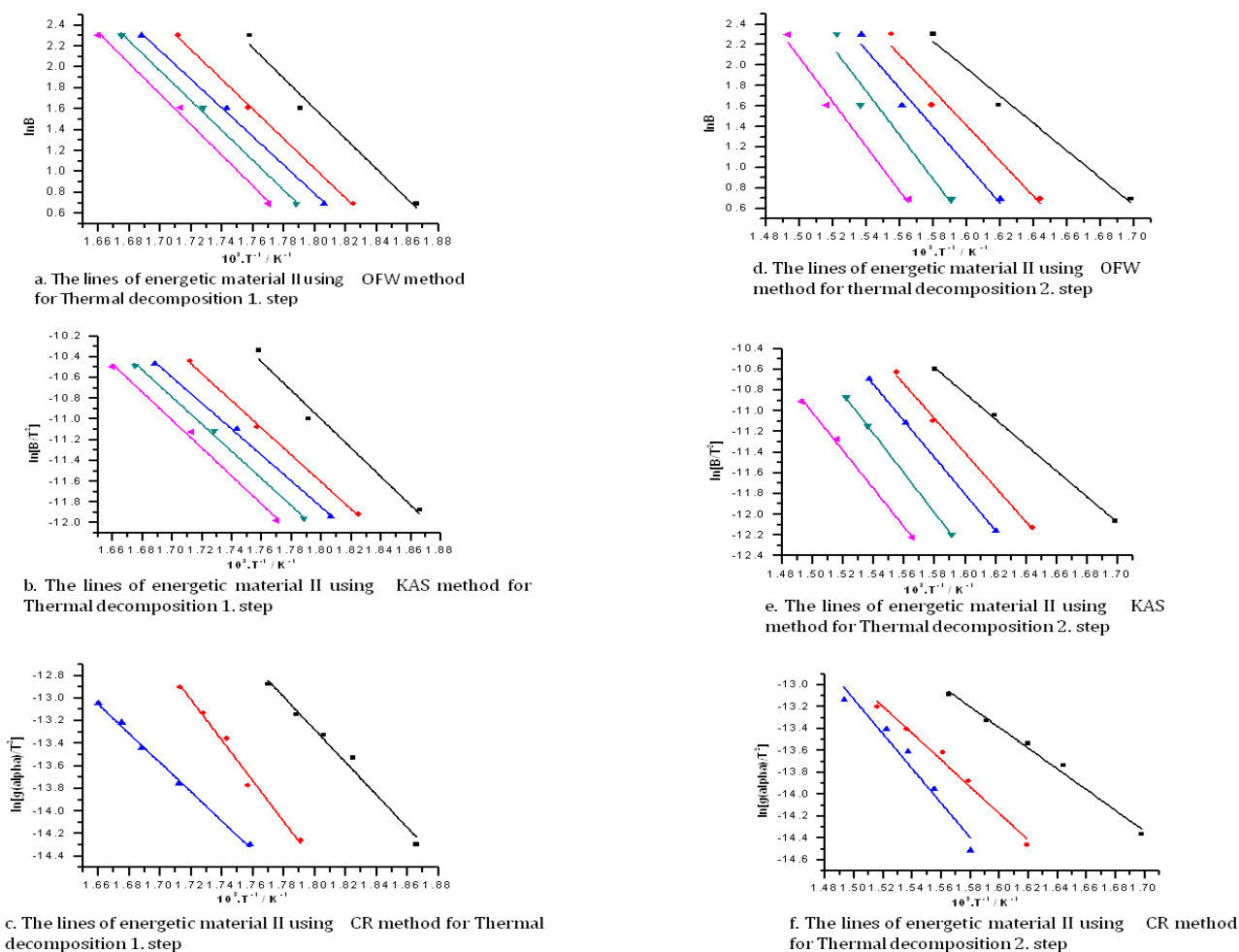


Figure 6. The lines obtained from the data of energetic material I for 1. And 2. thermal decomposition steps using OFW, KAS and CR methods. In the figure a, b, d and e black: $g(\alpha)=0.2$, red: $g(\alpha)=0.4$, blue: $g(\alpha)=0.5$, green: $g(\alpha)=0.6$, pink: $g(\alpha)=0.8$, in figure c and f black: heating rate: $0.5\text{ }^{\circ}\text{C}\cdot\text{min}^{-1}$, red: heating rate: $0.8\text{ }^{\circ}\text{C}\cdot\text{min}^{-1}$, blue: heating rate: $1.0\text{ }^{\circ}\text{C}\cdot\text{min}^{-1}$

For the energetic substance No I, the slopes of the curves on OFW graphic are positive at 0.5 , 0.8 and $1.0\text{ }^{\circ}\text{C}/\text{min}$. heating rates, as can be seen on Figure 5a. This makes measuring impossible. On the other hand, measuring can be done for KAS and CR equations. As the second thermal decomposition step of the energetic substance No I is very fast, there is an anomaly on the TFG curve obtained. Hence, no kinetic data could be obtained for the second thermal decomposition step of the energetic substance No I. Activation energies (E_a) and the Arrhenius pre-exponential factor (A) values obtained from the slopes and deviations of the of the above graphics are shown on Table 3. The thermodynamic parameters measured based on these values, are given on Table 4. In addition, Table 5 shows the rate constants measured for $g(\alpha)=0.4$, 0.5 and 0.6 where the reaction degree is considered to be $n=1$.

There is a single improper value among the values given on Table 4 obtained with the CR method at the first step of the thermal decomposition of the energetic substance No I, is the ΔS^0 value. This value is $371.88\text{ J}/\text{mole}$ and it is positive. As it is an explosion reaction, it does not seem reasonable for it

to be positive value. There is no external substance exchange and the products are gases. Thus, no entropy increase is expected in the environment. However, this is a somewhat extreme value as the A values obtained with the CR method are rather high. So, due to equation 4 ΔS^0 is measured high. There is no abnormal result between the rate constants that are measured based on the Arrhenius equation and given in Figure 5. Decomposition of these energetic substances occur in two steps. Only the first step of the energetic substance No. I can be measured. And this measuring can only be done at heating rates below $1\text{ }^{\circ}\text{C}\cdot\text{min}^{-1}$. The rate of the second step cannot be measured at these rates. The second step is also fast at $0.5\text{--}1.0\text{ }^{\circ}\text{C}\cdot\text{min}^{-1}$ heating rates and the data necessary for the measuring of kinetic parameters cannot be collected. Due to the fast rate of reaction, gases are produced suddenly and these gases immediately leave the environment due to the heat of the explosion, which causes a decrease in the ambient temperature and the pan temperature of the device decreases for a short while. In this case, the slope of the TG curve changes to positive from negative and thus, kinetic parameters cannot be measured at any kinetic equation. In addition, the measurements of

the first step of the thermal decomposition of this energetic substance could be done with the KAS and CR methods only. This is because in OFW method, the logarithmic value ($\ln\beta$) of the heating rate against the $1/T$ value are illustrated on graphics. Below $1^\circ\text{C}\cdot\text{min}^{-1}$ heating rate, $\ln\beta$ values are negative, which makes it impossible according to Equation 2, to measure the

E_a value as the slope = $-(E_a/R)$. When the slope is negative, E_a can be measured as positive. Thus, the $\ln\beta$ value must be positive to be able to use the OFW method and the heating rates must be above $1^\circ\text{C}\cdot\text{min}^{-1}$ for that. So it could be said that it is better to use the KAS method if the heating rates are below $1^\circ\text{C}\cdot\text{min}^{-1}$.

Table 3. The calculated E_a and A values of energetic material I and II from the graphs given in Fig. 5 and Fig. 6 for first and second step of their thermal decomposition separately

Energetic Material	Method					
	OFW		KAS		CR	
	E_a ($\text{kJ}\cdot\text{mol}^{-1}$)	A (min^{-1})	E_a ($\text{kJ}\cdot\text{mol}^{-1}$)	A (min^{-1})	E_a ($\text{kJ}\cdot\text{mol}^{-1}$)	A (min^{-1})
$\text{C}_5\text{H}_5\text{N}_5\text{O}_4$, N(3,5-dinitro-2-pyridyl)hydrazine (I) 1. thermal Step			$g(\alpha)=0.2$ 183.00±0.96 R=0.9988	6.70±0.08 10^{11}	$\theta=0.5$ 282.64±3.39 R=0.9949	8.31±0.23 10^{32}
			$g(\alpha)=0.4$ 142.92±2.71 R=0.9737	1.63±0.07 10^8	$\theta=0.8$ 275.79±4.83 R=0.9888	1.64±0.72 10^{32}
			$g(\alpha)=0.5$ 146.35±2.73 R=0.9778	4.39±0.18 10^8	$\theta=1.0$ 218.07±4.47 R=0.9759	6.88±0.32 10^{24}
			$g(\alpha)=0.6$ 139.98±3.16 R=0.9643	8.48±0.44 10^6	Average: 258.83±28.98	
			$g(\alpha)=0.8$ 122.66±2.56 R=0.9604	8.85±0.42 10^4		
			Average: 146.98±22.10			
$\text{C}_8\text{H}_6\text{N}_6\text{O}_4$, 2-N(pyrazol-3-yl)amino-3,5-dinitropyridyne (II) 1. thermal step	$g(\alpha)=0.2$ 120.07±2.45 R=0.9608	1.34±0.05. 10^7	$g(\alpha)=0.2$ 115.51±1.73 R=0.9806	15.56±0.52	$\theta=2.0$ 149.20±1.79 R=0.9822	8.16±0.17 10^{11}
	$g(\alpha)=0.4$ 117.89±0.62 R=0.9958	9.65±0.09. 10^6	$g(\alpha)=0.4$ 108.53±1.06 R=0.9973	4.47±0.04	$\theta=5.0$ 107.25±0.46 R=0.9954	2.30±0.03 10^{10}
	$g(\alpha)=0.5$ 113.58±0.63 R=0.9960	3.86±0.04. 10^6	$g(\alpha)=0.5$ 112.35±0.63 R=0.9966	1.60±0.02	$\theta=10.0$ 129.10±1.35 R=0.9763	4.87±0.10 10^{10}
	$g(\alpha)=0.6$ 118.60±0.75 R=0.9953	1.02±0.01. 10^7	$g(\alpha)=0.6$ 108.94±0.69 R=0.9931	4.46±0.05	Average: 128.52±17.39	
	$g(\alpha)=0.8$ 121.79±1.04 R=0.9917	2.44±0.03. 10^7	$g(\alpha)=0.8$ 112.08±0.97 R=0.9996	7.98±0.12		
	Average: 118.38±3.23		Average: 111.48±4.43			
$\text{C}_8\text{H}_6\text{N}_6\text{O}_4$, 2-N(pyrazol-3-yl)amino-3,5-dinitropyridyne (II) 2. thermal Step	$g(\alpha)=0.2$ 110.92±1.68 R=0.9937	1.99±0.05. 10^5	$g(\alpha)=0.2$ 103.89±0.38 R=0.9937	0.153±0.01	$\theta=2.0$ 78.67±0.45 R=0.9893	109.16±1.02
	$g(\alpha)=0.4$ 143.40±4.48 R=0.9986	9.16±0.46. 10^7	$g(\alpha)=0.4$ 138.27±1.10 R=0.9986	96.21±1.21	$\theta=5.0$ 101.56±0.85 R=0.9948	1.31±0.17 10^4
	$g(\alpha)=0.5$ 155.16±4.65 R=0.9745	6.93±0.33. 10^8	$g(\alpha)=0.5$ 146.68±0.02 R=0.9745	385.04±0.15	$\theta=10.0$ 131.30±2.36 R=0.9747	6.08±0.18 10^9
	$g(\alpha)=0.6$ 178.26±9.76 R=0.9877	3.49±0.30 10^{10}	$g(\alpha)=0.6$ 158.87±1.71 R=0.9877	2540.32±4.06	Average: 103.84±22.01	
	$g(\alpha)=0.8$ 181.07±4.98 R=0.9972	4.49±0.19. 10^{10}	$g(\alpha)=0.8$ 152.75±1.29 R=0.9972	665.84±8.65		
	Average: 153.76±27.05		Average: 140.09±18.01			

Considering the values given on Figure 5, for the heating rate of $\beta=5.0^\circ\text{C}/\text{min}$. used in the CR measurement of the thermal decomposition of the energetic substance No II, the rate constant of the first step was measured to be higher than the second step. In all the other measurements, the rate constant

of the second step was higher than that of the first step. This is right, as Figure 1 shows that the second step is faster than the first step for the energetic substance No I. The same could be expected for the energetic substance No II and in both the isoconversional and the nonisothermal methods

(OFW and KAS) the rate constant of the second step was higher than that of the first step. But in isothermal CR method, an opposite value at $\beta= 5.0$ °C/min. was found. This supports the suggestion offered by the International Confederation of Thermal Analysis and Calorimetry (ICTAC) in 2011. ICTAC advises that thermal kinetic measurements are done with nonisothermal-isoconversional methods [47].

In this study, antimicrobial activities of the energetic substances were measured with a different method. As explained in the experimental part, it was done based on 5 different types of bacteria and one fungus. The aim in this study is to define the antimicrobial properties of the energetic substances. Energetic substances probably have antimicrobial properties as

they are tense molecules. The tension on the cellular membrane or intracellular tension of the bacteria can have a negative effect on the reproduction of such bacteria. Antimicrobial activity was measured based on this consideration. The results are shown in Table 6. The values on Figure 6 show that neither of the two energetic substances demonstrates a high antimicrobial activity. They just have a slight impact on *B.suaptilis* and *S.aureus*. The energetic substance No II almost has no impact on the fungus (*C.albicans*). And on *E.Coli*, *E. Faecalis* ve *P.aeruginosa*, they can have impact at or above 256 ppm concentration only. These substances do not present a high antimicrobial activity mostly probably due to their nitrogen atoms. Nitrogen atoms outside the nitro groups, particularly the nitrogen atoms in the hetero ring act as a nutrient for the bacteria.

Table 4. The calculated Thermodynamic parameters of the energetic materials prepared from the graphical calculation

Energetic Material	Methods								
	OFW			KAS			CR		
	$\Delta H /$ kJ mole ⁻¹	ΔS J K ⁻¹	ΔG kJ mole ⁻¹	$\Delta H /$ kJ mole ⁻¹	ΔS J K ⁻¹	ΔG kJ mole ⁻¹	$\Delta H /$ kJ mole ⁻¹	ΔS J K ⁻¹	$\Delta G /$ kJ mole ⁻¹
C ₅ H ₅ N ₅ O ₄ , N(3,5-dinitro-2-pyridyl)hydrazine (I) 1. thermal Step				145.86*	-79.48	168.35	257.71	371.88	146.91
C ₈ H ₆ N ₆ O ₄ , 2-N(pyrazol-3-yl)amino-3,5-dinitropyridyne (II) 1. thermal step	116.27	-118.83	151.68	109.37	-241.03	181.19	126.40	-46.54	139.61
C ₈ H ₆ N ₆ O ₄ , 2-N(pyrazol-3-yl)amino-3,5-dinitropyridyne (II) 2. thermal Step	150.83	-75.67	172.45	137.16	-195.44	195.39	100.91	-166.10	150.40

Arrhenius pre-exponential factor values for $g(\alpha) = 0.5$ values and the mean value of the temperature range given in table 1 for ΔT were used in the calculations.

Table 5. The calculated rate constant values of the thermal decomposition reaction of energetic materials I and II on the first and second steps at $g(\alpha)=0.4 - 0.6$ and heating rate 5-10 °C.min⁻¹

Energetic Material	Methods								
	OFW			KAS			CR		
	k / min. ⁻¹ g(α)=0.4	k / min. ⁻¹ g(α)=0.5	k / min. ⁻¹ g(α)=0.6	k / min. ⁻¹ g (α)=0.4	k / min. ⁻¹ g(α)=0.5	k / min. ⁻¹ g(α)=0.6	k / min. ⁻¹	k / min. ⁻¹	k / min. ⁻¹
C ₅ H ₅ N ₅ O ₄ , N(3,5-dinitro-2-pyridyl)hydrazine (I) 1. thermal Step				8.54.10 ⁻¹⁰	3.14.10 ⁻¹⁰	7.84.10 ⁻⁷		θ=0.8 7.40.10 ⁻²	θ=1.0 2.94.10 ⁻²
C ₈ H ₆ N ₆ O ₄ , 2-N(pyrazol-3-yl)amino-3,5-dinitropyridyne (II) 1. thermal step	1.02.10 ⁻⁴	1.03.10 ⁻⁴	9.23.10 ⁻⁵	3.54.10 ⁻¹⁰	5.53.10 ⁻¹¹	3.20.10 ⁻¹⁰		θ=5.0 2.37	θ=10.0 4.64.10 ⁻²
C ₈ H ₆ N ₆ O ₄ , 2-N(pyrazol-3-yl)amino-3,5-dinitropyridyne (II) 2. thermal Step	2.86.10 ⁻⁴	2.46.10 ⁻⁴	1.74.10 ⁻⁴	7.73.10 ⁻¹⁰	6.54.10 ⁻¹⁰	4.55.10 ⁻¹⁰		θ=5.0 9.33.10 ⁻⁵	θ=10.0 0.177

Table 6. Minimum inhibition concentration (MIC) values of the energetic material prepared

1 (CE-1)	<i>E. coli</i>	<i>B. subtilis</i>	<i>E. faecalis</i>	<i>S. aureus</i>	<i>P. aeruginosa</i>	<i>C. albicans</i>
512 ppm	-	-	-	-	-	-
256 ppm	-	-	-	-	+	+
128 ppm	+	-	+	-	+	+
64 ppm	+	-	+	-	+	+
32 ppm	+	+	+	+	+	+
16ppm	+	+	+	+	+	+
8 ppm	+	+	+	+	+	+
2 (CE-2)						
512 ppm	-	-	+	-	+	+
256 ppm	+	-	+	-	+	+
128 ppm	+	-	+	-	+	+
64 ppm	+	-	+	+	+	+
32 ppm	+	-	+	+	+	+
16ppm	+	+	+	+	+	+
8 ppm	+	+	+	+	+	+

4. Discussion and Conclusion

Two new energetic substances prepared by nucleophilic substitution reactions were studied by using chloro dinitro pyridine. As they involved amino and nitro groups at ortho position, they were thermally decomposed in two steps with a furoxane ring-like sub-product. Results of the TG studies and kinetic analysis showed that the second step reaction was faster than the first one. The two steps of one of the energetic substances could be individually observed at ordinary heating rates, whereas the second step couldn't be observed in the decomposition of the other energetic substance at ordinary heating rates. Thus, much lower heating rates were used and the second step could be observed. Only the first step of this energetic substance was studied with the kinetic models. No mathematical measurement was made for the second step. Besides, as the logarithm of the heating rate was negative, the kinetic analysis of the first step of the reaction was not measured with the OFW method, but rather with the KAS and CR methods. It was concluded that, the KAS method would be better when the heating rate was below $1^{\circ}\text{C}\cdot\text{min}^{-1}$.

References

[1] Huheey JF, The electronegativity of multiply bonded groups, *J. Phys. Chem.* 1966;70:2086-91.
 [2] Agrawal JP, Surve RN, Sonawane SH. Some aromatic nitrate esters: Synthesis, Structural aspects, thermal and explosive properties. *J. Hazard. Mat.* 2000;77:11-31.
 [3] Agrawal JP, Hodgson RD. *Organic Chemistry of explosives.* Chichester :Wiley;2007. P.158-62.

[4] Yiğiter AÖ, Atakol MK, Aksu ML, Atakol O. Thermal characterization and theoretical and experimental comparison of picryl chloride derivatives of heterocyclic energetic compounds. *J. Therm. Anal. Cal.* 2017;127:2199-2123.

[5] Badgujar D.M, Talawar M.B, Harlapur S.F, Asthana S.N, Mahulikar P.P. Synthesis, characterization and evaluation of 1,2-bis(2,4,6-trinitrophenyl)hydrazine. *J. Hazard. Mat.* 2009;172:276-279.

[6] Agrawal J.P. Past, Present & Future of Thermally Stable Explosives. *Central Eur. J. Energ. Mat.* 2013;9:273-290.

[7] Chiato ZL, Klapötke TM, Mieskes F, Stierstörfer J, Weyrauther M. (Picrylamino)-1,2,4-triazole Derivatives-Thermally stable explosives, *Eur. J. Inorg. Chem.* 2016;956-62.

[8] Agrawal J.P. *High Energy Materials.* Wiley-VCH Verlag GmbH. 2010;93-95.

[9] Klapötke T.M. *Chemistry of High-Energy Materials.* Walter de Gruyter. 2012;pp.141-61.

[10] Tao GH, Parrish DA, Shreeve JM. Nitrogen rich 5-(1-Methylhydrazinyl)tetrazole and its copper and silver complexes. *Inorg. Chem.* 2012;51:5305-12.

[11] Politzer P, Murray J. S. *Decomposition, Crystal and Molecular Properties. Energetic Materials.* Amsterdam.2003;Part 1:411-416.

[12] Talawar MB, Sivabalan R, Mukundan T, Muthurajan H, Sikder AK, Gandhe BR, Rao AS. Environmentally compatible next generation green energetic materials. *J. Hazard. Mat.* 2009;161:589-607.

- [13] Bailey A.S, Case J.R. 4:6-dinitrobenzofuroxan, nitrobenzodifuroxan and benzotrifuroxan: A new series of complex-forming reagents for aromatic hydrocarbons. *Tetrahedron* 1958;3:113-131.
- [14] Reddy G.O, Murall B.K.M, Chotterjee A.K. Thermal study on picryl azide (2-azido-1,3,5-trinitrobenzene) decomposition using simultaneous thermogravimetry and differential scanning calorimetry. *Propellants, Explosives, Pyrotechnics*. 1983;8:29-33.
- [15] Kehler J, Püschl A, Dahl O. Improved Syntheses of 1-Hydroxy-4-nitro-6-trifluoromethylbenzotriazole and 1-Hydroxy-4,6-dinitrobenzotriazole. *Acta Chim. Scandinavica* 1996;50:1171-73.
- [16] Özkaramete, E, Şenocak N, K. İnal E.K, Öz S. Svoboda I, Atakol O. Experimental and computational studies on the thermal degradation of nitroazidobenzenes, propellants, explosives, pyrotechnics. 2013;38:113-119.
- [17] Cardillo P, Gigante L, Lunghi A, Zanirato P. Revisiting the thermal decomposition of five ortho-substituted phenyl azides by calorimetric technics, *J. Therm. Anal. Cal.* 2010;100:191-198.
- [18] Shremetev A.B, Aleksandrova N.S, Ignat N.V, Schulte M. Straightforward one-pot synthesis of benzofuroxans from o-halonitrobenzenes in Ionic Liquids. *Mendeleev Comm.*2012;22:95-97.
- [19] Brown ME. Introduction to Thermal analysis. Kluwer Academic Publishers, 2001;p.206.
- [20] Kraynikova A, Rotaru A, Györyova K, Homzova K, Manolea HO, Kavarova J, Hudecova D. Thermal behaviour and antimicrobial assay of some new zinc(II) 2-aminobenzoate complex compound with bioactive ligands. *J. Therm. Anal. Cal.* 2015;120:73-83.
- [21] Abdelouahed L, Leveneur S, Vernieres-Hassimi L, Balland L, Taouk B. Comparative investigation for the determination of kinetic parameters for biomass pyrolysis by thermogravimetric analysis. *J. Therm. Anal. Cal.*2017;129:1201-13.
- [22] Sarada K, Muraleedharan K. Effect of addition of silver on the thermal decomposition kinetics of copper oxalate. *J. Therm. Anal. Cal.* 2016;123:643-51.
- [23] Kullyakool S, Siritwong K, Noisong P, Danvirutai C. Kinetic triplet evaluation of a complicated dehydration of $\text{Co}_3(\text{PO}_4)_2 \cdot 8\text{H}_2\text{O}$ using the deconvolution and simplified master plots combined with nonlinear regression. *J. Therm. Anal. Cal.* 2017;127:1963-74.
- [24] Suekkhayad A, Noisong P, Danvirutai C. Synthesis, thermodynamic and kinetic studies of the formation of LiMnPO_4 from a new $\text{Mn}(\text{H}_2\text{PO}_2)_2 \cdot \text{H}_2\text{O}$ precursor. *J. Therm. Anal. Cal.* 2017;129:123-34.
- [25] Moine EC, Bouamoud R, El Hamidi A, Khachani M, Halim M, Arsalane S. Mineralogical characterization and non-isothermal pyrolysis kinetics of Moroccan Rif oil shale. *J. Therm. Anal. Cal.* 2018;131:993-1004.
- [26] Pouretedal HR, Mousavi SL. Study of the ratio of fuel to oxidant on the kinetic of ignition reaction of $\text{Mg}/\text{Ba}(\text{NO}_3)_2$ and $\text{Mg}/\text{Sr}(\text{NO}_3)_2$ pyrotechnics by non-isothermal TG/DSC technique. *J. Therm. Anal. Cal.* 2018; DOI:10.1007/s10973-018-7028
- [27] Jarayaman K, Kök MV, Gökalp İ. Combustion properties and kinetics of different biomass samples using TG-MS technique. *J. Therm. Anal. Cal.* 2017;127:1361-70.
- [28] Pouretedal HR, Damiri S, Ravanbod M, Hagsdost M, Masoudi S. The kinetic of thermal decomposition of PETN, Pentastite and Pentolite by TG/DTA non-isothermal methods. *J. Therm. Anal. Cal.* 2017;129:521-29.
- [29] Ravanbod M, Pouretedal HR. Catalytic effect of Fe_2O_3 , Mn_2O_3 and TiO_2 nanoparticles on thermal decomposition of potassium nitrate. *J. Therm. Anal. Cal.* 2016;124:1091-98.
- [30] Koga N. Qzawa's kinetic method for analyzing thermoanalytical curves. *J. Therm. Anal. Cal.* 2013;113:1527-41.
- [31] Abdel-Kader NS, Amin RM, El-Ansary AI. Complex of Schiff base of benzopyran-4-one derivative. *J. Therm. Anal. Cal.* 2016;123:1695-1706.
- [32] Naktiyok J, Bayrakçeken H, Özer AK, Gülaboğlu MŞ. Investigation of combustion kinetics of Umutbaca-lignite by thermal analysis technique. *J. Therm. Anal. Cal.* 2017;129:531-39.
- [33] Ganeshan G, Shadangi KP, Mohanty K. Degredation kinetic study of pyrolysis and co-pyrolysis of biomass with polyethylene terephthalide (PET) using Coats-Redfern method. *J. Therm. Anal. Cal.* 2018;131:1803-16.
- [34] Ebrahimi HP, Hadi JS, Abdulnabi ZA, Bolandnazar Z. Spectroscopic, thermal analysis and DFT computational studies of salen -type Schiff base complexes. *Spectrochimica Acta* 2014;117:485-92.
- [35] Gaussian 09, Revision D.01. Gaussian Inc. Wallingford CT, USA, 2009.
- [36] Ochterski J. W., Petersson Jr. G. A, Montgomery Jr. J. A., *J. Chem. Phys.* 104 (1996)2598.
- [37] Montgomery J. A., Frisch M. J., Ochterski J. W., Petersson G. A., *J. Chem. Phys.* 112 (2000) 6532.
- [38] Gökçınar E., Klapötke T. M., Bellamy A. J., *J. Mol. Struct.* 953 (2010) 18-23.
- [39] Politzer P., Lane P., Concha M. C., *Struct. Chem.* 15 (2004) 468-79.
- [40] Liu QR, Xue LW, Zhao GQ, Manganese(III) Complexes Derived from bis-Schiff Bases. *Russian J. Coord. Chem.* 2014; 40:757-63.
- [41] Montazerzohari M, Jahromi SM, Masoudiasl A, McArdle P. Nanostructure zinc(II) Schiff Base

complexes of a N-3-tridentate ligand as new biological active agents. *Spectrochim. Acta A*. 2015; 138:517-28.

[42] Gaelle DSY, Yufanyi DM, Jagan R, Agwara MO. Synthesis, Characterization and Antimicrobial Activity of cobalt(II) and cobalt(III) complexes derived from 1,10-Phenanthroline with nitrate and azide co-Ligands. *Cogent Chemistry* 2016; 2: Article number: 1253201; DOI: 10.1080/23312009.2016.1253201.

[43] Atakol M, Atakol A, Yiğiter AÖ, Svoboda I, Atakol O. Investigation of energetic materials prepared by reactions of diamines with picrylchloride. *J. Therm. Anal. Cal.* 2017;127:1931-40.

[44] Şen N, Özkaramete E, Yılmaz N, Öz S, Svoboda I, Akay A, Atakol O. Thermal decomposition of dinitrochloro-azido benzenes. *J. Energ. Mat.* 2014;32:75-9.

[45] Klapötke TM. *Chemistry of High Energy Materials*. Walter de Gruyter 2012;p75-79.

[46] Kubota N, *Propellants and Explosives*. Wiley-VCH Verlag GmbH & Co. KGaA 2007;p.36.

[47] Vyazovkin S, Burnham AK, Criado JM, Perez-Magueda LA, Popescu C, Sbirazzuoli N. ICTAC Kinetics Committee recommendations for performing kinetic computations on thermal analysis data. *Thermochim. Acta* 2011;520:1-19.